Historical Contingency Shapes Toxin Resistance in a Specialist Avian Predator

Author List:
Mohammadi, S. [1, 2], Pradhan, S. [1], Hoffmann, F. G. [3, 4], Herrera-Álvarez, S. [5], Deng, Y. [6], Eacock, A. [1], Dobler, S. [2], Storz, J. F. [7], Rowland, H. M. [1,8]

Author Affiliations:
[1] Max Planck Institute for Chemical Ecology, Research Group Predators and Toxic Prey, Jena, Germany
[2] Molecular Evolutionary Biology, Institute of Cell and Systems Biology of Animals, Universität Hamburg, Hamburg, Germany
[3]Department of Biochemistry, Nutrition, and Health Promotion, Mississippi State University, Mississippi State, MS 39762, USA
[4]Institute for Genomics, Biocomputing, and Biotechnology, Mississippi State University, Mississippi State, MS 39762, USA
[5]Department of Ecology and Evolution, University of Chicago, Chicago, IL, USA
[6] BGI-Shenzhen, Shenzhen 518083, China
[7] School of Biological Sciences, University of Nebraska, Lincoln, NE, USA
[8] Department of Evolution, Ecology, and Behaviour, Institute of Infection, Veterinary, and Ecological Sciences, University of Liverpool, UK

Contact Information: Shabnam Mohammadi (smohammadi@ice.mpg.de) and Hannah M. Rowland (hrowland@liverpool.ac.uk)

Keywords: Black-headed grosbeak, Na,K-ATPase, cardiac glycosides, toxin resistance, protein evolution, ancestral sequence reconstruction.

Summary

Adaptations to toxic diets can cascade through ecosystems, altering physiology, species interactions, and trophic dynamics. To uncover the molecular basis of toxin resistance in the black-headed grosbeak (*Pheucticus melanocephalus*), a specialist predator of cardiotonic steroid-defended monarch butterflies (*Danaus plexippus*), we investigated the evolution of target-site insensitivity in the toxin's molecular target – the Na,K-ATPase. Functional assays of engineered Na,K-ATPases revealed that resistance in grosbeaks arises from a non-additive interaction between a substitution at position 111 (Q111E) and up to six nearby amino acid changes in the first extracellular loop of the protein. Using resurrected ancestral proteins, we show that the earliest of these six substitutions to evolve (V113L) altered the functional effects of Q111E, such that Q111E alone became maladaptive. Only after the accumulation of additional permissive substitutions could Q111E confer resistance, highlighting how intramolecular epistatic interactions and historical contingency constrained the evolutionary path to adaptation. Our phylogenetic analysis of Na,K-ATPase sequences from 360 birds further revealed that several of the specific grosbeak substitutions—particularly at sites 112, 114, and 116—show strong signatures of co-evolution with changes at site 111 across the avian tree, supporting the hypothesis that resistance evolves through repeated, interacting changes. Together, these results reveal the molecular mechanisms of convergent evolution of toxin resistance and demonstrate how genetic background can shape evolutionary outcomes across trophic levels.

21 **Introduction**

22 Cardiotonic steroids (CTSs) are a diverse class of toxins found in plants, insects, and
23 vertebrates [1, 2]. They are highly toxic to most animals because they bind to and inhibit the
24 α subunit of the Na,K-ATPase (ATP1A1), a transmembrane ion pump that is essential for
25 maintaining membrane potentials and cellular function [3, 4]. The black-headed grosbeak
26 (*Pheucticus melanocephalus*), a migratory songbird that breeds in western North America
27 and winters in Mexico [5], exhibits a rare and highly specialised predatory behaviour. These
28 birds prey on overwintering adult monarch butterflies (*Danaus plexippus*) in the Oyamel fir
29 forests of central Mexico [6]. These butterflies are defended by CTS toxins [6, 7]. In mixed-
30 species flocks with black-backed orioles (*Icterus galbula abeillei*), black-headed grosbeaks
31 can kill up to 15,000 monarchs per day across the overwintering sites [8]. Analyses of
32 grosbeak stomach contents have found CTS quantities as high as 259ug (equivalent to
33 6.17 mg/kg; [7]), and the birds can tolerate oral doses of 1050 mg/kg [6] – a level exceeding
34 the lethal dose (LD_{50}) of other CTSs tested in mice [9-13]. This remarkable resistance to CTSs
35 has been suggested to be a further example of convergent molecular evolution in target-site
36 insensitivity in the Na,K-ATPase [14, 15], a pattern documented in other vertebrates such as
37 murid rodents, neotropical grass frogs, and snakes that feed on CTS-defended prey [16-18].
38

39 The molecular basis of CTS resistance has repeatedly evolved through amino acid
40 substitutions in the first extracellular loop of Na,K-ATPase, which forms a critical region of
41 the toxin's binding pocket [16, 18-22]. Following this pattern, the black-headed grosbeak
42 has a glutamine-to-glutamic acid substitution in the same loop at position 111 (Q111E). This
43 amino acid site has been identified as a hotspot for major-effect substitutions that confer
44 target-site insensitivity of Na,K-ATPase to CTS in several insect and vertebrate species [23,
45 24]. In addition to Q111E, there are five other amino acid changes in the grosbeak's first
46 extracellular loop – S112T, M114V, E115N, E116G, and P118G. This differentiates the
47 grosbeak from its closest relative with an available genome sequence the Lazuli bunting
48 (*Passerina amoena*) and from other species of birds that do not prey on monarchs (Fig. 1).
49 L113, another substitution in the first extracellular loop distinguishes the grosbeak and
50 other songbirds (Passeriformes) from most other species of birds, except for the Abyssinian
51 ground hornbill (*Bucorvus abyssinicus*), which is also reported to feed on CTS-defended prey
52 [25]. If these substitutions are responsible for the grosbeak's ability to specialise on

53 monarchs, the adaptation would represent a rare example of an evolutionary cascade [15,
54 26], whereby plant-derived toxins in monarchs drive selective pressures that extend to the
55 third trophic level, shaping species far removed from the primary toxin source and,
56 ultimately, species interactions across trophic levels.

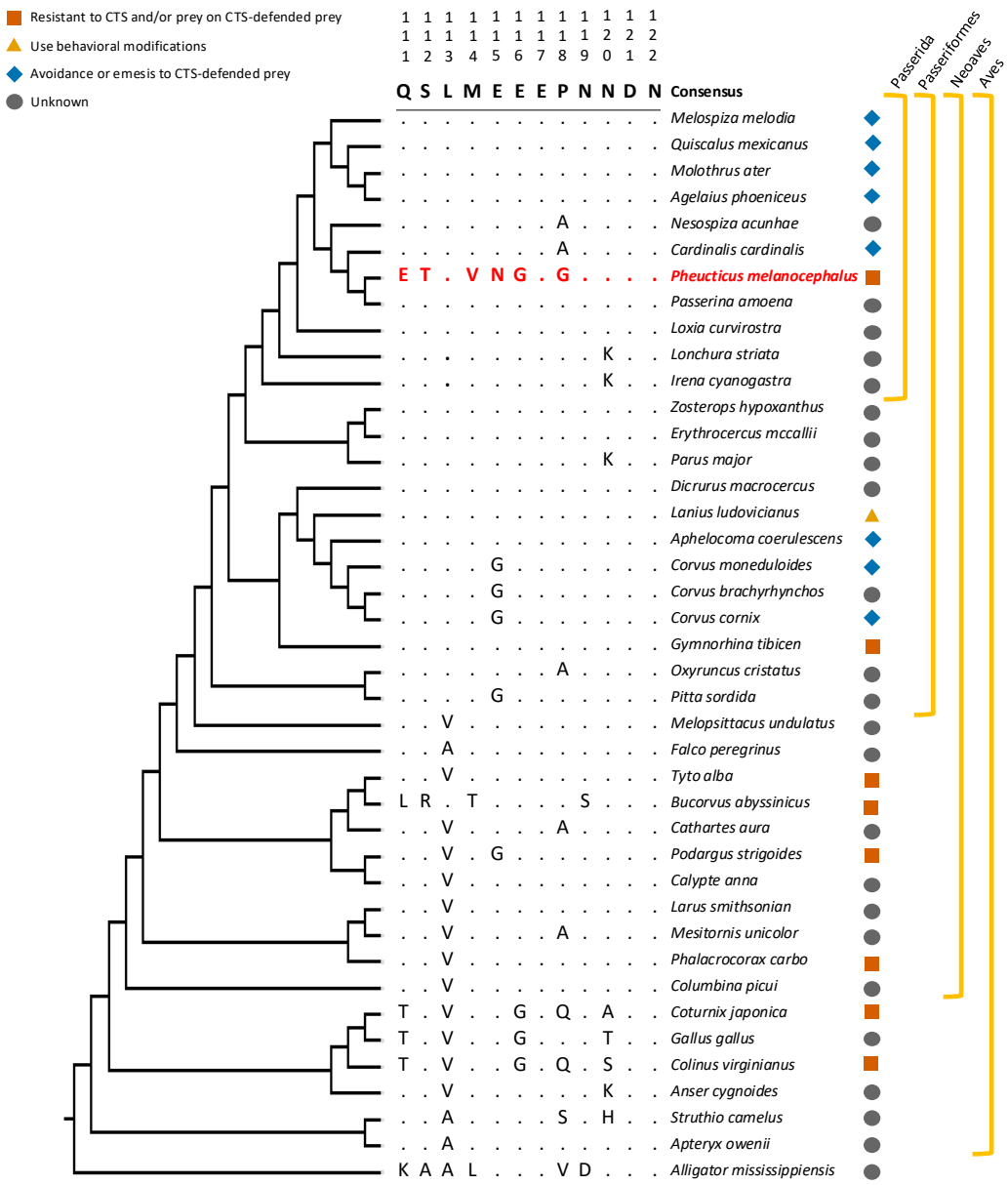

57

58 **Figure 1.** A phylogenetic subtree of birds showing amino acid differences in the first
59 extracellular loop of the Na,K-ATPase α1 subunit (ATP1A1), a key target of CTSs. Amino acid
60 positions are numbered according to the sheep (*Ovis aries*) reference sequence, following
61 convention. Differences from the consensus sequence (not the inferred ancestral sequence)
62 are shown for each species. Coloured symbols to the right of each species indicate the

63 reported response of each species to CTS-defended prey: blue diamond – species that
64 exhibit avoidance or emesis (vomiting) in response to CTS-defended prey; yellow triangle –
65 species that use behavioural adaptations to feed on CTS-defended prey; orange square –
66 species that show no emetic response when fed CTS-defended prey and/or have been
67 observed feeding on CTS-defended prey or plants; grey circle – species for which no
68 published data are available regarding CTS sensitivity or tolerance.
69
70 **Results and Discussion**
71 We used protein engineering experiments to address the following questions about the
72 grosbeak's Na,K-ATPase. (1) Is Q111E a major-effect substitution that is necessary and
73 sufficient to confer target-site insensitivity? (2) Does the set of associated substitutions
74 (T112A, L113A, V114M, N115E, G116E, and G118P; hereafter referred to as 6subs) also
75 contribute to target-site insensitivity? (3) do these additional substitutions compensate for
76 deleterious effects of Q111E on overall protein function, rather than directly contributing to
77 target-site insensitivity? To address these questions, we used heterologous protein
78 expression and biochemical assays to quantify the functional effects of engineered variants
79 in the Na,K-ATPase. Using the wildtype grosbeak Na,K-ATPase as a starting point, we
80 synthesised four Na,K-ATPase constructs in which the Q111E and 6subs substitutions were
81 individually or jointly reverted to their inferred ancestral state. For each engineered protein
82 we measured resistance as the concentration of CTS (ouabain) at which enzyme activity is
83 reduced to 50% (i.e., IC50) and assessed overall protein activity by quantifying the rate at
84 which the enzyme hydrolyses ATP.
85
86 Consistent with the hypothesis that Q111E is a major-effect substitution with respect to
87 target-site insensitivity, reverting that site to the ancestral amino acid state (E111Q)
88 significantly reduced resistance in wildtype grosbeak Na,K-ATPase. We also found that
89 reverting the amino acid states of 6subs significantly reduced resistance compared to the
90 wildtype protein, though this reduction was significantly less pronounced than the effect of
91 E111Q alone. Reverting Q111E and 6subs in tandem did not produce any further reduction
92 in resistance relative to that produced by either reversion alone (Table S2, Fig. 2A). While
93 our results clearly demonstrate the presence of target-site insensitivity in the grosbeak

94 Na,K-ATPase, they also reveal that the resistance-conferring effects of E111 are conditional
95 on the presence of additional amino acid substitutions within the extracellular loop.
96
97 That reverting Q111E and the associated 6subs together does not reduce resistance beyond
98 either reversion alone indicates a non-additive interaction, likely due to intramolecular
99 epistasis. Similar nonadditive effects of resistance-conferring mutations have been
100 documented in other systems of target-site insensitivity to CTS [16, 18]. For example,
101 introducing E111 into the *Drosophila* Na,K-ATPase conferred only a tenfold increase in
102 resistance, whereas the addition of a second substitution, Y122 (as found in aphids), led to
103 more than a hundredfold increase in resistance [27]. In contrast to most previously studied
104 systems, where epistasis typically involves two key sites (primarily positions 111 and 122),
105 the grosbeak Na,K-ATPase shows conditional effects involving up to six interacting
106 substitutions. This represents a more complex and unique evolutionary trajectory within a
107 system otherwise characterised by highly repeatable molecular adaptations [28].
108
109 Functional investigations of CTS resistance-conferring substitutions in the Na,K-ATPase of
110 other resistant species have revealed they often have negative pleiotropic effects on native
111 activity (the rate at which the enzyme hydrolyses ATP), and such effects are sometimes
112 mitigated by compensatory substitutions at other sites in the proteins [16, 18, 23, 24]. If the
113 amino acid changes that confer CTS resistance in the grosbeak Na,K-ATPase negatively
114 impact the protein's other functions, we would predict that the individual reversions of
115 Q111E and 6subs would produce a significant increase in protein activity relative to the
116 wildtype grosbeak ATP1A1 genotype. Our experimental results show that this is not the
117 case. Reverting Q111E and 6subs individually and in combination reduced protein activity
118 (Fig. 2B; Table S2). The increased resistance to CTS in the grosbeak Na,K-ATPase is therefore
119 associated with increased protein activity, which suggests that the mutation(s) conferring
120 resistance also enhance or stabilise enzyme efficiency. In contrast to the compensatory
121 amino acid interactions documented in the Na,K-ATPases of other CTS-resistant taxa [16, 18,
122 23, 24, 29], our experiments on grosbeak Na,K-ATPase provide no evidence that the
123 resistance conferred by Q111E compromises native activity [16, 18, 23, 24, 29].
124

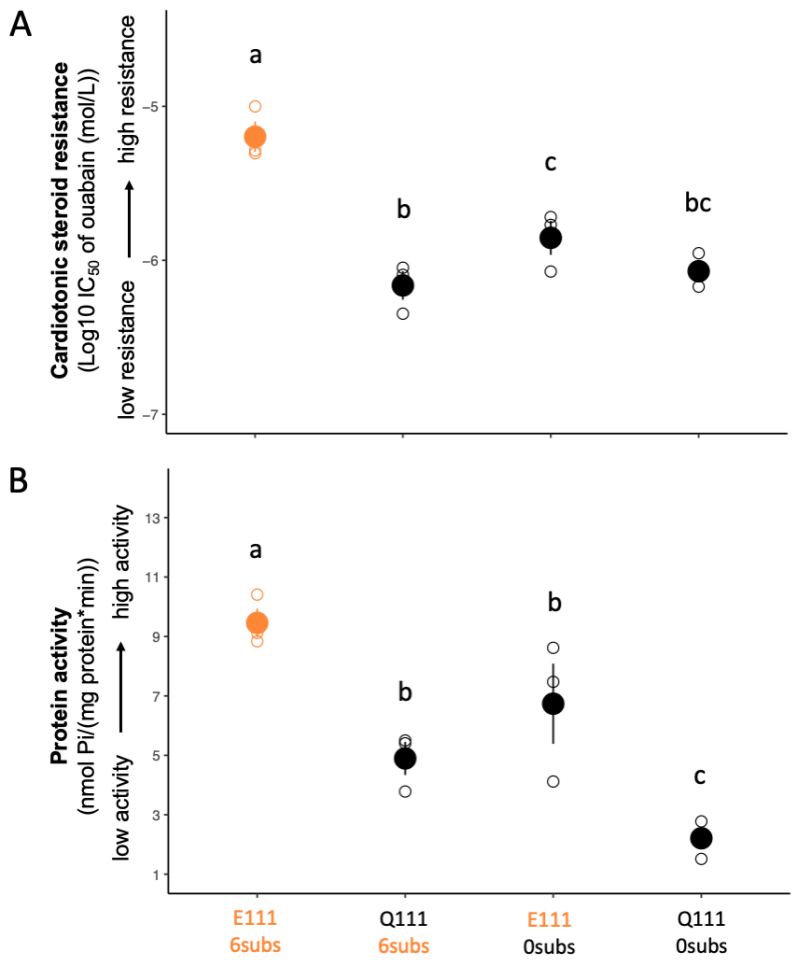

Figure 2. Functional effects of reverting grosbeak-specific Na,K-ATPase substitutions into their ancestral states, individually and in combination. For each recombinant protein, the substitutions were generated on the modern grosbeak genetic background and the resulting amino acid states are denoted on the x-axis. Amino acid states that are wildtype on the modern grosbeak Na,K-ATPase are given in orange and those that are ancestral in black. Panel A shows cardiotonic steroid resistance (i.e., mean $\log_{10}IC_{50}$ ± SEM) plotted on the y-axis. Panel B shows the corresponding protein activity (i.e., mean ATP hydrolysis rate ± SEM) for the same proteins plotted on the y-axis. Raw data from three biological replicates are shown as open circles. Significant differences between proteins (contrast analysis) are indicated by different letters.

That E111's resistance-conferring effects depend on the presence of multiple other substitutions indicates that the path to target-site insensitivity was constrained by earlier molecular changes. To determine whether historical contingency played a role in shaping

140 the evolution of CTS resistance in grosbeaks, we statistically reconstructed and
141 experimentally resurrected a set of progressively more ancient Na,K-ATPase constructs
142 representing a temporal sequence of ancestral genotypes from three points in the grosbeak
143 line of descent. These three points represent (1) the common ancestor of all birds (AncAves,
144 150–165 Mya [30] (Fig. 3A); (2) the common ancestor of Neoaves (AncNeoaves, 67.4 Mya
145 [31]), an incredibly diverse groups of modern birds, including waterfowl (Anseriformes),
146 shorebirds (Charadriiformes), raptors (Accipitriformes), and songbirds (Passeriformes); and
147 (3) the common ancestor of Passerida (AncPasserida, 22.4 Mya [31]), a large and diverse
148 clade (or infraorder) within the order Passeriformes, which includes finches, warblers,
149 thrushes, sparrows, swallows, and larks. We selected AncPasserida as the most recent
150 common ancestor of modern grosbeaks and other core passerines, rather than the common
151 ancestor with *Passerina amoena* (the grosbeak's closest sequenced relative), based on the
152 hypothesis that the grosbeak's specialised foraging behaviour on CTS-defended prey is an
153 older rather than a more recent adaptation [32]. AncPasserida also provides a more
154 conservative baseline for identifying derived substitutions in the grosbeak lineage (Table
155 S3).
156

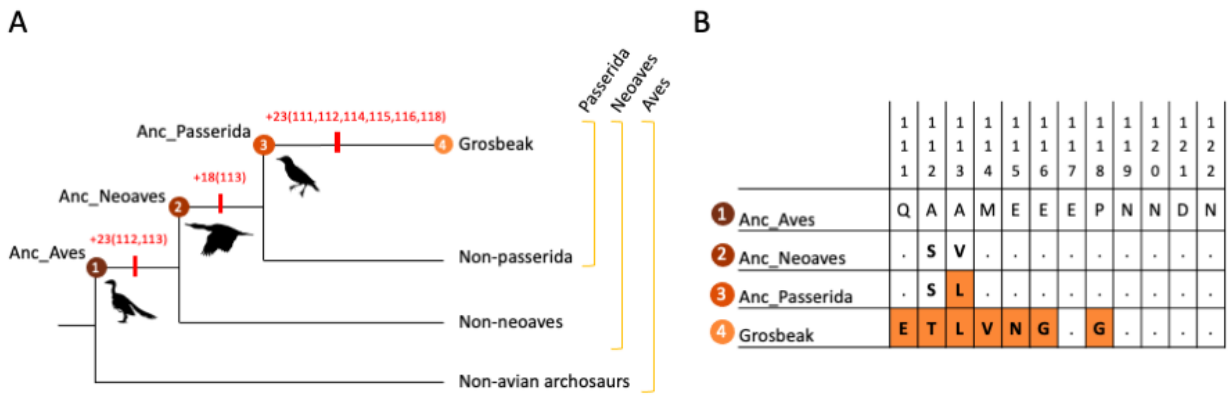

157
158 **Figure 3.** (A) A schematic phylogeny tracing the line of descent of the black-headed
159 grosbeak back to the most recent common ancestor of all birds (AncAves). We
160 reconstructed three ancestral steps along this lineage: ancestral Aves (node 1), ancestral
161 Neoaves (node 2), and ancestral Passerida (node 3). From AncAves to the modern grosbeak,
162 a total of 47 amino acid substitutions were gained in the Na,K-ATPase α1-subunit (encoded
163 by the ATP1A1 gene). Of these substitutions, 23 (including A112S and A113V in the first

164 extracellular loop) occurred on the branch connecting AncAves to AncNeoaves, 18 occurred
165 on the branch connecting AncNeoaves to AncPasserida (including V113L), and 23 occurred
166 on the branch connecting AncPasserida to the ATP1A1 of contemporary grosbeaks
167 (including Q111E and the five remaining changes comprising 6subs; Fig. 3B). (B) Seven of
168 these 47 substitutions (highlighted in orange) are in the protein's first extracellular loop,
169 which spans amino acid sites 111 to 122 and makes up a critical region of the toxin's binding
170 pocket.
171
172 We assessed whether the resistance-conferring substitutions found in modern grosbeaks
173 would have had similar phenotypic effects in progressively more ancient ATP1A1 genotypes
174 along their evolutionary lineage. To do this, we synthesised and heterologously expressed
175 AncPasserida, AncNeoaves, and AncAves with and without the modern grosbeak
176 substitutions Q111E and 6subs. By comparing the effects of Q111E and 6subs on these
177 ancestral backgrounds, each progressively more divergent from the wildtype ATP1A1
178 genotype of contemporary grosbeaks, we tested how genetic context modulates the
179 functional impact of these mutations
180
181 We found that toxin resistance conferred by Q111E alone was ancestrally accessible, but its
182 effect diminished and eventually reversed as the mutation was moved onto increasingly
183 more recent ancestral backgrounds (Fig. 4A; Table S4). Q111E caused a significant increase
184 in resistance on the AncAves protein (Fig. 4A, left panel; Table S4). Q111E's positive effect
185 on resistance decreased when the mutation was introduced into the more recent
186 AncNeoaves protein, which differs from AncAves by two substitutions (A112S and A113V) in
187 the first extracellular loop. Subsequently, with the emergence of V113L in AncPasserida –
188 the most recent ancestral background – the effect of Q111E reversed, shifting from
189 resistance-increasing to resistance-decreasing (Fig. 4A, left panel; Table S4).
190
191 Because V113L was the first substitution of the grosbeak's 6subs to arise in AncPasserida,
192 we investigated its potential role in altering the effect of Q111E. To do this, we synthesised
193 and expressed an alternative AncPasserida, engineered to carry Q111E along with a
194 reversion of V113L (i.e., L113V; a new version of AncNeoaves with 17 additional
195 substitutions outside of the first extracellular loop; Fig 4A, white bar in left panel). This

196 approach allowed us to isolate the effect of V113L in its immediate historical context, while
197 preserving all other substitutions separating AncNeoaves from AncPasserida, and thus
198 enabling a focused test of its functional role in modulating Q111E. We confirmed that
199 introducing the V113L substitution reversed the effect of Q111E, changing its impact from
200 increasing to decreasing CTS resistance (Fig. 4A, left panel; Table S4). This significant
201 functional alteration between AncNeoaves and AncPasserida demonstrates the crucial role
202 of V113L in the evolutionary transition to the modern grosbeak genotype. The fixation of
203 V113L seems to have restricted the subsequent evolution of Q111E, potentially
204 necessitating the fixation of the additional five substitutions in the modern grosbeak. This
205 underscores how genetic context and epistatic interactions can shape the accessibility of
206 adaptive mutations, and how mutations that are initially deleterious can become beneficial
207 again through subsequent permissive or compensatory changes.
208
209 To test how the functional effects of 6subs changed over time, we introduced them into the
210 three reconstructed ancestral backgrounds. On the most ancient background, AncAves,
211 6subs had no significant effect on CTS resistance (Fig 4A, middle panel). On AncNeoaves,
212 they slightly decreased resistance—an effect that was slightly stronger than the resistance-
213 decreasing effect of Q111E alone on AncPasserida. In contrast, on AncPasserida, 6subs
214 produced a significant increase in resistance (Fig 4A, middle panel). Thus, despite V113L
215 reversing Q111E's effect in AncPasserida, 6subs still conferred CTS resistance with or
216 without Q111E. When Q111E and 6subs were introduced together, they consistently
217 produced a significant increase in CTS resistance across all ancestral backgrounds (Fig. 4A,
218 right panel; Table S4).
219
220 These findings illustrate how epistatic interactions shaped the emergence of resistance:
221 both Q111E and 6subs could contribute to CTS resistance, but their effects varied with
222 genetic context. This suggests a distinctive form of historical contingency in the protein's
223 evolution, in which intramolecular epistasis locks in the effects of certain beneficial
224 mutations by making their functional impact dependent on the presence of earlier
225 substitutions. Such interactions can open otherwise inaccessible evolutionary pathways,
226 enabling the gradual assembly of complex, adaptive phenotypes like CTS resistance.
227

228 To further understand the evolutionary dynamics of these substitutions, we investigated
229 whether there were functional trade-offs between toxin resistance and protein activity,
230 which could have influenced the fixation of the modern grosbeak substitutions. Across all
231 ancestral backgrounds, we found that Q111E has a minor negative effect on protein activity
232 (Fig. 4B left panel; Table S4). In contrast, 6subs had consistently positive effects on protein
233 activity when introduced on ancestral backgrounds, with significant effects on the
234 AncPasserida and AncAves backgrounds *(*Fig. 4B, middle panel; Table S4). These results
235 suggest that the evolution of CTS resistance via 6subs alone would have likely led to an
236 increase in protein activity. When combined, Q111E and 6subs produced a mix of positive
237 and negative effects on protein activity depending on the genetic background (Fig. 4B, right
238 panel; Table S4). The combination had a neutral to negative effect on protein activity in
239 AncAves and AncNeoaves, but significantly increased activity in the more recent
240 AncPasserida background (Table S4; Fig. 4B right panel; Table S4). This positive effect of the
241 combined substitutions on activity in AncPasserida aligns with the negative effect of
242 reverting these mutations in the modern grosbeak. Our results suggest that the epistatic
243 interaction between Q111E and 6subs balances the trade-off between CTS resistance and
244 native protein activity, providing further evidence that intramolecular epistasis facilitated
245 the evolutionary assembly of the resistant genotype in the grosbeak. We confirmed that
246 functional inferences were robust to statistical uncertainties in ancestral reconstruction
247 (Table S6).

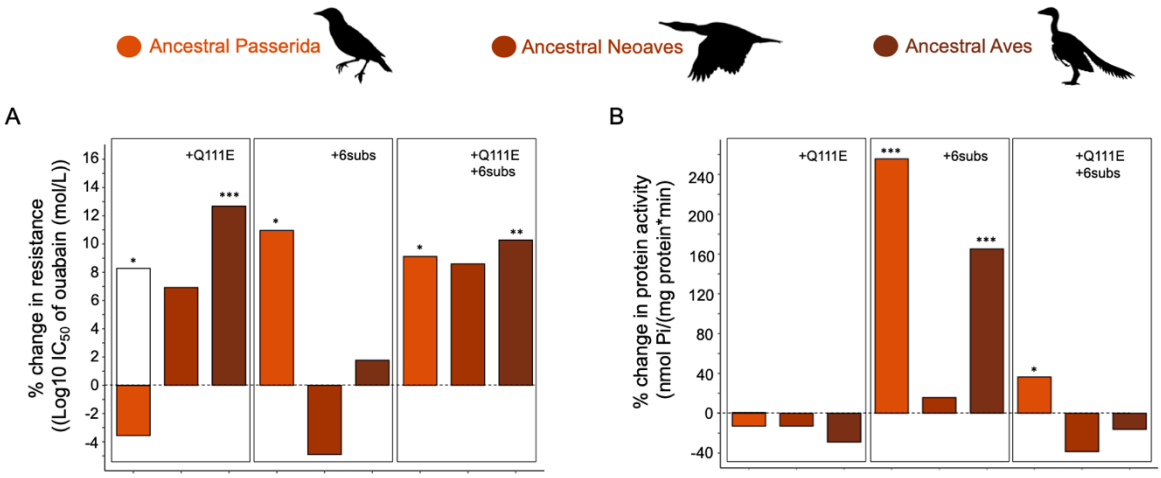

248

249 **Figure 4.** Functional properties of engineered Na,K-ATPases measuring the effects of

250 modern black-headed grosbeak substitutions on increasingly more ancient genetic
251 backgrounds (from orange to maroon). The graphs in panels A and B show the percent
252 change in functional properties of wildtype ancestral NKAs in comparison to their
253 mutagenised counterpart. Each set of bars (from left to right) shows the effects of one of
254 three substitutions or sets of substitutions (Q111E, 6subs, and Q111E+6subs). In panel A, a
255 measure of CTS resistance (i.e., mean $\log_{10}IC_{50}$ ± SEM from three biological replicates) is
256 plotted on the y axis. In panel B, a measure of protein activity (i.e., mean ATP hydrolysis rate
257 ± SEM from three biological replicates) for the same proteins is plotted on the y axis.
258 Significant differences (contrast analysis; Table S5, Fig. S1) between wildtype and
259 mutagenised proteins are indicated by asterisks. In the Q111E graphs are an additional
260 mutagenised construct of ancestral Passerida, engineered to carry Q111E as well as L113V.
261 This additional construct is illustrated by a white bar. In panel B, this white bar completely
262 overlaps with the original and is therefore not visible. Significance codes: 0 '***'; 0.001 '**';
263 0.01 '*'.
264
265 Our functional experiments established that the evolution of target-site insensitivity in the
266 modern grosbeak Na,K-ATPase involved nonadditive interactions between Q111E and
267 6subs. To assess evidence for interactions between Q111E and individual substitutions
268 comprising 6subs in grosbeaks, we investigated phylogenetic patterns of co-variation in
269 amino acid states across the Na,K-ATPases orthologs of class Aves. We built a phylogeny of
270 full-length ATP1A1 sequences of 360 birds and created a comprehensive catalogue of amino
271 acid variation among birds (Fig. 5). Notably, Q111E has evolved independently at least seven
272 times across distinct bird lineages, including the *Tinamiformes* (tinamous),
273 *Cuculiformes* (cuckoos), *Psittaciformes* (parrots), *Trogoniformes* (trogons),
274 *Galliformes* (game birds), and *Musophagiformes* (turacos). The grosbeak is the only songbird
275 (*Passeriformes*) so far identified to have this substitution [33].
276
277 Given that the avian ATP1A1 sequence is extremely well conserved across all species (mean
278 branch length of 0.0037 substitutions per site), we investigated whether the Q111E
279 substitution consistently co-occurs with other (potentially compensatory) substitutions in
280 different lineages. Site 114, which is among the six substitutions comprising 6subs, was one
281 of the eight sites whose substitution patterns fall within the top 5% for coevolutionary signal

282 with Q111E (Fig. 5; Fig. S2). The substitution M114V in the grosbeak has evolved
283 independently in a cockatoo clade where Q111E is also fixed. Further, all the closest
284 relatives of the grosbeak that are known to be sensitive to the toxin retain the ancestral
285 state at site 114 (Fig. 1; Fig. 5).
286
287 We expanded our coevolution analysis to identify additional sites that could be contributing
288 to the evolution of target-site insensitivity in the grosbeak. We relaxed the coevolution
289 analyses to identify other sites with substitutions that show a non-random co-occurrence
290 with changes at position 111, regardless of whether that change is to glutamate (E) or
291 another amino acid. This leverages the fact that site 111, which is involved in the
292 convergent evolution of target-site insensitivity across vertebrates [16], has repeatedly
293 experienced substitutions across the avian phylogeny (at least 13 times; Fig. 5). Among the
294 5% sites with strongest coevolution signals with site 111, two sites – 112 and 116 – are part
295 of 6subs (Fig. S3). The substitution S112T in the grosbeak, for example, occurs
296 independently in the same cockatoo clade that carries M114V, while all the closest relatives
297 of the grosbeak maintain the ancestral state at site 112. These results suggest that epistatic
298 interactions between Q111E, S112T, M114V, and E116G also contribute to the evolution of
299 target-site insensitivity in the grosbeak.
300

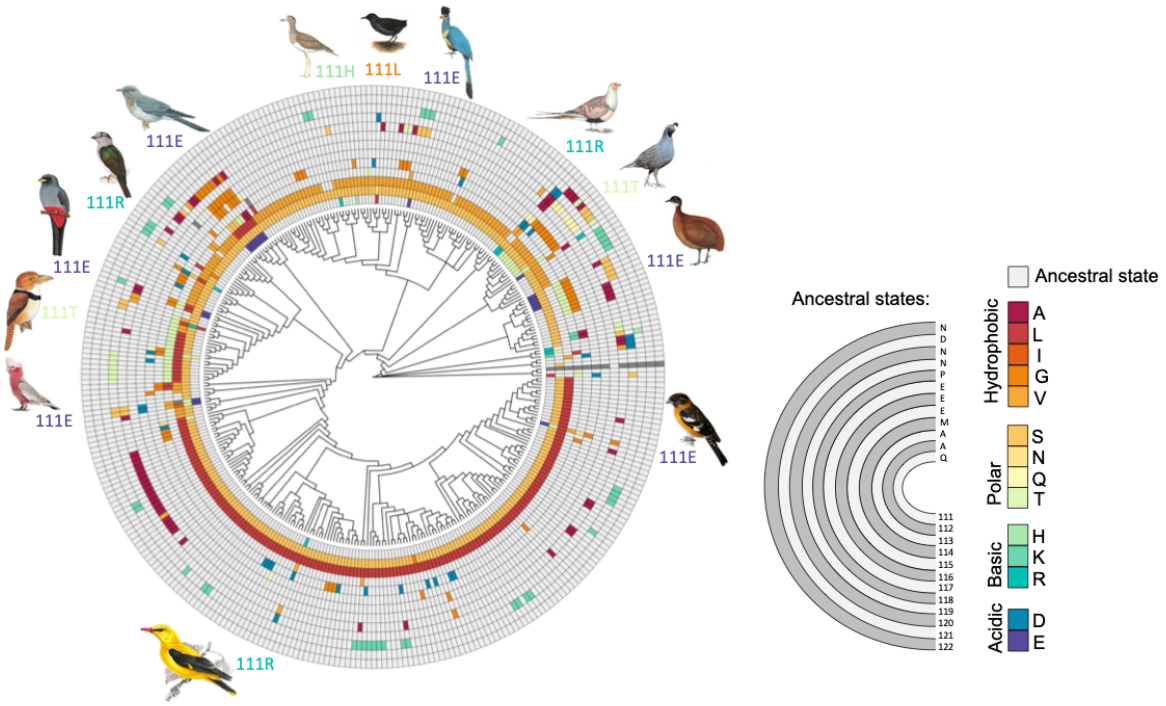

Figure 5. Circular phylogeny of birds showing amino acid states of the H1–H2 loop of the Na,K-ATPase ATP1A1 gene. Mutations within the H1–H2 loop have been associated with target-site insensitivity of the enzyme towards cardiotonic steroids, especially at sites 111 and 122. Notable substitutions are illustrated around the phylogeny.

The conditional effects of multiple substitutions in the grosbeak Na,K-ATPase represent a unique evolutionary outcome within this broader pattern of repeated adaptation [16, 20, 23, 24, 28, 34]. In contrast, other species such as horned frogs (*Ceratophrys*) and garter snakes (*Thamnophis*), both of which prey on CTS-containing toads, have independently evolved alternative resistance mechanisms involving a single amino acid substitution [16]. Similarly, the yellow-throated sandgrouse (*Pterocles gutturalis*) has developed a distinct single-amino acid insertion in the H1–H2 extracellular loop, a modification also associated with CTS resistance in pyrgomorphid grasshoppers [35-37]. These examples emphasise how different species have achieved the same functional outcome – resistance to CTS – through distinct molecular solutions, highlighting the diversity of adaptive strategies across species and trophic levels, and the complexity of evolutionary pathways to the convergent evolution of toxin resistance.

Resource Availability

Lead Contact: Further information and requests on methods can be directed to Dr. Hannah M. Rowland and Dr. Shabnam Mohammadi.

Materials Availability: Plasmids used in this study have been deposited in Addgene (see Key Resources Table for names and numbers). This study did not generate new unique reagents.

Data and Code: Data and code generated during this study are available through links provided in the Key Resources Table. Sequence data for ATP1A1 and ATP1B1 were obtained from genome assemblies under BioProject PRJNA545868 [38].

Acknowledgements

We thank Guojie Zhang and Josefin Stiller for initial discussions and subsequent access to the genomic resources under BioProject PRJNA545868 [38]. We thank J. Stiller, M. Winters, K. Rohlfing, M. Röpcke, and K. Otto for critical reading of drafts of this manuscript. We thank V. Wagschal, C. Plate, F. Miazzi, and K. Barthold for assistance in the laboratory. This research was funded by the Max Planck Society to HMR.

Author Contributions

Conceptualisation: SM, JFS, HMR; **Methodology:** SM, FGH, SHA, AE, SD, JFS, HMR; **Software**: SM, FGH, SHA, YD, HMR; **Validation:** SP; **Formal analysis:** SM, SP, FGH, SHA, YD, HMR; **Investigation:** SM, FGH, SHA, YD; **Resources:** FGH, SD; **Data Curation**: SM, SP, FGH, AE, HMR; **Writing - Original Draft**: SM, HMR; **Writing - Review & Editing:** SP, FGH, SHA, YD, AE, SD, JFS; **Visualization:** SM

Declaration of Interests

The authors declare no competing interests.

347 **Key Resources Table**

348

Reagent or Resource	Source	Identifier
Bacterial and Virus Strains		
Escherichia coli MAX Efficiency™ DH10Bac Competent Cells	Thermo Fisher Scientific	Cat#10361012
Escherichia coli XL 10-Gold Competent Cells	Agilent Technologies, La Jolla, CA, USA	Cat#200314
Experimental Models: Cell Lines		
Insect: Sf9 cells in Sf-900™ II SFM	Thermo Fisher	Cat#11496015
Technical devices		
Ultrasonic homogeniser Sonopuls 2070	Bandelin Electronic Company, Berlin, Germany	
Centrifuge 5840 R	Eppendorf AG, Hamburg, Germany	
Ultra-Centrifuge L-80	Beckmann Coulter GmbH, Krefeld, Germany	
Freeze dryer Alpha 1-2 LD plus	Martin Christ Gefriertrocknungsanlagen GmbH, Osterode am Harz, Germany	
Ultrasonic homogeniser Omni Sonic Ruptor 400	Omni International Inc., Kennesaw, GA, USA	
Cuvette spectrophotometer Ultrospec 2100 pro	Amersham Biosciences Europe GmbH, Freiburg im Breisgau, Germany	
Microplate shaker BioShake iQ	Quantifoil Instruments, Jena, Germany	
Microplate absorbance reader Bio-Rad Model 680 Bio-Rad iMark (spectrophotometers and software package)	**Bio-Rad Laboratories GmbH,** Feldkirchen, Germany	
96-well polystyrene flat-well plate	SARSTEDT AG & Co. KG, Nümbrecht, Germany	Cat#82.1581
Chemicals, Peptides, and Recombinant Proteins		
Insect-Xpress medium	Lonza, Walkersville, MD, USA	Cat#BE12-730P10
Gentamycin	Roth, Karlsruhe, Germany	Cat#0233.1
PEI MAX	Polysciences Inc., Warrington, PA, USA	CAS#49553-93-7
HPLC grade water ROTIPURAN p.a., ACS water	Roth, Karlsruhe, Germany	Cat#HN68.2
Bovine serum albumin (BSA)	Roth, Karlsruhe, Germany	CAS#90604-29-8

Nitrocellulose membrane	Roth, Karlsruhe, Germany	Cat#HP42.1
BlueBlock PF	SERVA Electrophoresis GmbH, Heidelberg, Germany	Cat#42591.01
4-Chloro-1-naphthol	Merck KGaA, Darmstadt, Germany	Cat#C8890
Tween 20	Merck KGaA, Darmstadt, Germany	CAS#9005-64-5
3,3',5,5'-tetramethylbenzidine (TMB)	Thermo Fisher Scientific Inc., Rockford, IL, USA	Cat#N301
Parafilm	Merck KGaA, Darmstadt, Germany	Cat#P7793
Ouabain octahydrate, 96%	Thermo Fisher Scientific Inc., Rockford, IL, USA	CAS#11018-89-6
Adenosin-5-triphosphat Bis-(Tris)-salt hydrate (ATP)	Merck KGaA, Darmstadt, Germany	CAS#102047-34-7
Antibodies		
α5-antibody (primary antibody)	Developmental Studies Hybridoma Bank, University of Iowa, Iowa City, IA, USA	RRID: AB_2166869
HRP-antibody (secondary antibody conjugated with horseradish peroxidase)	Dianova, Hamburg, Germany	RRID: AB_2617176
Deposited Data		
Raw data for recombinant Na,K-ATPase functional assays	This paper	Dryad doi: https://doi.org/
ATP1A1 and ATP1B1 alignments and associated phylogenetic trees used to generate ancestral sequence reconstructions	This paper	Dryad doi: https://doi.org/
R scripts and associated data tables used for statistical analyses and generating figures	This paper	Dryad doi: https://doi.org/
Recombinant DNA		
All plasmids generated in this study are listed in Table S1	This paper	See Table S1
Software		
R	https://www.r-project.org/	R version 4.1.1

349

350 **Methods**

351

352 **Ancestral protein reconstruction**. We compiled a dataset of avian ATP1A1 (n=370 species)

353 and ATP1B1 (n=365 species) sequences from high-coverage genome assemblies (BioProject

354 PRJNA545868 [38]) together with online sequences from nine reptiles [39-41]. Ancestral
355 reconstruction was conducted on 343 ATP1A1 and 340 ATP1B1 sequences. Sequences were
356 aligned using the MAFFT alignment algorithm [42], and ancestral reconstruction was
357 estimated using the maximum likelihood (ML) approach implemented in IQ-TREE v 2.1.2
358 [43], with the aid of the Lazarus set of Python scripts for parsing results [44]. We
359 constructed supertrees for avian sequences based on phylogenies corresponding to the
360 most well-supported understanding of the species tree at the time of analysis [45-47].
361 Insertions were manually removed from marginal reconstructions, and ATP1A1 and ATP1B1
362 sequences of three ancestral NKAs in the grosbeak lineage were reconstructed and
363 subsequently synthesised: AncAves, AncNeoaves, and AncPasserida. We also reconstructed
364 and synthesised alternative ancestral reconstructions for altAncAves and altAncNeoaves by
365 substituting sites with posterior probabilities below 0.8 when the ratio of the top two
366 probabilities was less than 4:1. These alternative constructs were functionally assayed
367 alongside the best estimates to confirm that minor uncertainty did not affect inferred
368 function (Table S6). All sites in AncPasserida had posterior probabilities above 0.8, so no
369 alternatives were generated.
370
371 **Construction of expression vectors**. ATP1A1 and ATP1B1 genes of each recombinant NKA
372 construct were synthesised (Invitrogen GeneArt) and codon optimised for *Spodoptera*
373 *frugiperda.* The genes were cloned in pFastBac Dual (PFBD) plasmid with ATP1B1 under p10
374 promoter and ATP1A1 under P_{PH} promoter and confirmed by sequencing. The plasmid
375 constructs were fully sequenced and deposited in the Addgene repository under accession
376 numbers 196450 and 196454–70.
377
378 **Generation of recombinant viruses and transfection into Sf9 cells (*Spodoptera frugiperda*).**
379 *Escherichia coli* DH10bac cells harboring the baculovirus genome (bacmid) and a
380 transposition helper vector (Thermo Fisher Scientific; Cat#10361012) were transformed
381 using a modified protocol of the manufacturer's protocol with expression vectors containing
382 the different gene constructs. Recombinant bacmids were selected using the blue-white
383 screening method in agar plates containing kanamycin (50 µg/ml), gentamycin (7 µg/ml),
384 tetracycline (10 µg/ml), X-gal (100 µg/ml) and IPTG (40 µg/ml). Positive (white) colonies
385 were confirmed by PCR using the M13 primers (Forward primer: 5'-

386 CCCAGTCACGACGTTGTAAAACG-3', Reverse primer: 5'-AGCGGATAACAATTTCACACAGG-3') as
387 recommended by the manufacturer.
388
389 **Preparation of Sf9 membranes.** Baculovirus-mediated transfection was performed using a
390 modified protocol as described by Scholz and Suppmann [48]. Transfection mix was
391 prepared in 100 µl PBS with 10 µg recombinant bacmid and 20 µl PEI-MAX (1mg/ml) per
392 biological replicate. After 30 min of incubation, the transfection mix was added to actively
393 growing Sf9 cells (8×106 cells/ml) in 10 ml of Insect-Xpress medium (Lonza; Cat#BE12-
394 730P10) with 30 µg/ml gentamycin. Transfected cells were incubated at 27°C and 120rpm,
395 and amplified viruses were harvested after 5 days by pelleting and discarding the cells (P0
396 virus stock). 500 µl of P0 virus stock was added to 5×10^6 Sf9 cells/ml in 50ml Insect-Xpress
397 media with 30 µg/ml gentamycin and cultured at 27°C and 120rpm in 250 ml conical flasks
398 for 72h. Following incubation, Sf9 cells were harvested by centrifugation at 1650 × g for 10
399 min and the resulting cell pellets were immediately stored at –80°C.
400
401 **Membrane isolation from Sf9 cells.** Frozen pellets were homogenised in 15ml
402 homogenisation buffer (0.25 M sucrose, 2 mM ethylenediaminetetraacetic acid, and 25 mM
403 HEPES/Tris; pH 7.0) on ice. Cell suspension was sonicated at 60 W (Sonopuls 2070; Bandelin
404 Electronic Company, Berlin, Germany) for three 45 s intervals on ice. The cell suspension
405 was then centrifuged for 30 min at 10,000 × g (J2-21 centrifuge, Beckmann-Coulter, Krefeld,
406 Germany) at 4°C to remove debris. The supernatant was collected and further centrifuged
407 for 60 min at 146,000 × g at 4°C (Ultra- Centrifuge L-80, Beckmann-Coulter) to pellet the cell
408 membranes. The pelleted membranes were washed twice and resuspended in 1ml
409 ROTIPURAN p.a., ACS water (Roth; Cat#HN68.2) and stored at −20 °C. Three biological
410 replicates of each construct were used to conduct functional assays and protein
411 concentrations were determined by ELISA.
412
413 **Protein Quanitification and Verification by ELISA and SDS-PAGE/western blotting.** For the
414 ELISA, we followed the protocol as described by Löptien et al.[49]. First, 100 µL of
415 membrane isolates and relative standards were added to a 96-well polystyrene, slightly
416 hydrophilic flat-well plate (Immulon 2 HB, Thermo Fisher Scientific, Massachusetts, USA;
417 Cat#6302) in duplicate (two technical replicates). The standards were prepared from an

418 aliquot of lyophilised *Pheucticus melanocephalus* membrane isolate as described by Löptien
419 et al [49]. The plate was sealed and incubated overnight at 4°C (12–18 h). The next day, non-
420 coated leftovers were removed from the wells and washed five times with washing buffer
421 (Phosphate-buffered saline – 137 mM NaCl, 1.47 mM KH_2PO_4, 7.749 mM Na_2HPO_4,
422 2.683 mM KCl with 0.05 % Tween 20). Next, non-specific binding sites were blocked by
423 adding 200 µL of blocking buffer (1% BSA in PBS + 0.02% Tween 20) and incubating at room
424 temperature for 2 h. Following the blocking, the wells were washed another five times.
425 NKAs were detected by adding 50 µL of primary antibody solution containing 2 µg/mL
426 antibody (α5-antibody; Developmental Studies Hybridoma Bank, University of Iowa, Iowa
427 City, IA, USA; RRID: AB_2166869) in blocking buffer incubating for 1 h at room temperature,
428 then washed five times. To detect the primary antibody, 50 µL of secondary antibody
429 solution containing 10 µg/mL HRP-conjugated goat-anti-mouse antibody (HRP-antibody;
430 Dianova, Hamburg, Germany; RRID: AB_2617176) in blocking buffer was added and
431 incubated for 1 h at room temperature. Following secondary antibody incubation, wells
432 were washed seven times. The secondary antibody was stained by adding 100 µL
433 3,3',5,5' tetramethylbenzidine (TMB; Merck/Sigma-Aldrich; Cat#T4444) to each well, and
434 then left to incubate at room temperature for 10 mins. Staining was stopped by adding 100
435 µL 0.5 M sulfuric acid to each well. The OD was read at 495 nm using a plate reader (BioRad
436 Model 680 spectrophotometer and software package).
437
438 For the western blot, we followed the protocol described by Löptien et al.[49] In brief, 5 µL
439 of protein were solubilised overnight in 8 µL 4 × Laemmli buffer (62.5 mM Tris HCl pH 6.8; 2
440 % SDS; 10 % glycerol; 5 % 2-mercaptoethanol; 0.001 % Bromophenol Blue) and 19 µL
441 Millipore water, then separated on SDS gels containing 10% acrylamide. They were then
442 blotted on nitrocellulose membrane (HP42.1, Roth). After blotting, the membrane was
443 incubated with 1 × BlueBlock PF for 1 h. After blocking, the membranes were incubated at
444 room temperature with the primary monoclonal antibody α5 (Developmental Studies
445 Hybridoma Bank, University of Iowa, Iowa City, IA, USA) for 1.5 hours. Since only membrane
446 proteins were isolated from transfected cells, detection of the α subunit also indicates the
447 presence of the β subunit. The primary antibody was detected using a goat-anti-mouse
448 secondary antibody conjugated with horseradish peroxidase (Dianova, Hamburg, Germany).
449 The staining of the precipitated polypeptide-antibody complexes was performed by

450 repetitively pipetting the detecting substrate (0.035 % H_2O_2, and 0.01 % 4-Chloro-1-
451 naphthol in 0.05 M, pH 7.5 Tris HCl) over the membrane. See Figure S4.
452
453 **Ouabain inhibition assay**. To determine the sensitivity of each NKA construct to the water-
454 soluble cardiotonic steroid ouabain (Ouabain octahydrate 96%; Acrōs Organic;
455 Cat#AC161730010s), 100 ug of each protein was pipetted into each well in a nine-well row
456 on a 96-well flat-bottom microplate containing stabilising buffers (see buffer formulas in
457 [34]. The first six wells in a nine-well row were exposed to exponentially decreasing
458 concentrations of ouabain (10^{-3} M, 10^{-4} M, 10^{-5} M, 10^{-6} M, 10^{-7} M, 10^{-8} M, dissolved in
459 distilled H_2O). The seventh well was exposed to HPLC-grade water only (experimental
460 control). The eighth well was exposed to an inhibition buffer lacking KCl and containing 10^{-}
461 ^{2}M ouabain (ouabain octahydrate 96%; Acrōs Organic; Cat#AC161730010s), which
462 completely inhibits the NKA's ATPase activity and therby allows measurement of
463 background ATPase activity (see Petschenka et al.[34]). The proteins were incubated at 37°C
464 and 200 rpms for 10 minutes on a microplate shaker (BioShake iQ; Quantifoil Instruments,
465 Jena, Germany; Cat#1808-0506). Next, ATP (Adenosin-5-triphosphat Bis-(Tris)-salt hydrate;
466 Merck/Sigma-Aldrich; CAS#102047-34-7) was added to each well and the proteins were
467 incubated again at 37°C and 200 rpm for 20 minutes. The activity of Na,K-ATPases following
468 ouabain exposure was determined by quantification of inorganic phosphate (Pi) released
469 from enzymatically hydrolysed ATP. Reaction Pi levels were measured according to the
470 procedure described by Taussky and Shorr [50] (see Petschenka et al [34]). All assays were
471 run in duplicate and the average of the two technical replicates was used for subsequent
472 statistical analyses. Two constructs were run in Absorbance for each well and were
473 measured at 650 nm with a plate absorbance reader (BioRad Model 680 spectrophotometer
474 and software package).
475
476 **ATP hydrolysis assay.** To determine the functional efficiency of different Na,K-ATPase
477 constructs, we calculated the amount of Pi hydrolysed from ATP per mg of protein per
478 minute. The measurements were obtained from the same assay as described above. In
479 brief, absorbance from the experimental control reactions, in which 100 ug of protein was
480 incubated without any inhibiting factors (i.e., ouabain or buffer excluding KCl), was
481 measured and translated to mM Pi from a standard curve that was run in parallel (1.2 mM

482 Pi, 1 mM Pi, 0.8 mM Pi, 0.6 mM Pi, 0.4 mM Pi, 0.2 mM Pi, 0 mM Pi). ATP hydrolysis
483 measurements were always taken after the second freeze-thaw of each sample.
484
485 **Statistical analyses.** Background phosphate absorbance levels from reactions with inhibiting
486 factors were used to calibrate phosphate absorbance in wells measuring ouabain inhibition
487 and in the control wells [34]. For ouabain sensitivity measurements, calibrated absorbance
488 values were converted to percentage non-inhibited protein activity based on measurements
489 from the control wells [34]. These data were plotted and $\log_{10}$ IC_{50} values were obtained for
490 each biological replicate from nonlinear fitting using a four-parameter logistic curve, with
491 the top asymptote set to 100 and the bottom asymptote set to zero. Curve fitting was
492 performed with the nlsLM function of the minipack.lm library in R. For comparisons of
493 protein activity, the calculated Pi concentrations of protein assayed in the absence of
494 ouabain were converted to nmol Pi/mg protein/min. IC_{50} values were $\log_{10}$-transformed
495 prior to analysis to better meet the assumptions of normality and homogeneity of variance.
496 All statistical analyses were implemented in R. Data were plotted using the ggplot2 package
497 in R.
498
499 We first analysed the effects of substitutions in the modern grosbeak NKA. We ran a 2-way
500 ANOVA to assess the main effects of point mutations and their interaction, followed by
501 planned contrasts to identify significant differences between recombinant proteins (Table
502 S2). We then used linear regression to estimate the effect sizes of the explanatory variables
503 and to assess their additive and nonadditive effects (Table S2). In a second set of analyses,
504 we determined the background dependence of substitutions (i.e., interaction between
505 genetic background and amino acid substitution) with respect to CTS resistance (log10 IC_{50})
506 and ATPase activity (Table S5). Specifically, we tested whether the effects of a substitution X
507 -> Y are equal on different backgrounds (null hypothesis: X->Y (background 1) = X->Y
508 (background 2)). All statistical analyses were implemented in R. Data were plotted using the
509 ggplot2 package in R.
510
511 **Identifying correlated substitutions.** We used BayesTraits [51] to detect sites across the
512 ATP1A1 bird phylogeny that exhibit correlated evolution with substitution Q111E or site
513 111, hereafter referred to as substitution and site models, respectively. Using the

514 reconstructed ancestral sequence for the avian ATP1A1, we recoded each amino acid state
515 among extant sequences of the multi-species alignment into ancestral ‘0’ and derived ‘1’
516 states and used these and the phylogeny with estimated branch lengths as inputs for
517 BayesTraits. For the substitution model, site 111 was recoded as ‘1’ only for lineages that
518 have 111E fixed; for the site model, site 111 was recoded as ‘1’ in every lineage with a
519 substitution at this site (e.g., Q111X). These model specifications allowed us to use
520 BayesTraits to fit a continuous-time Markov model to estimate transition rates between
521 discrete, binary traits and estimate the best fitting model describing their joint evolution on
522 a phylogeny. We excluded singleton sites and sites with more than 80% gaps, as these sites
523 would be of little information. This resulted in an analysis of 144 variant sites.
524
525 With the substitution model, we tested whether the rate at which the substitution Q111E
526 occurs was dependent on all other variant sites; with the site model, we tested whether the
527 rate of evolution at site 111 was dependent on all other variant sites. Both coevolution
528 models have a null independent and an alternative dependent model. The null independent
529 model assumes that the two sites evolve independently, and the alternative dependent
530 model assumes that the sites are correlated such that the change at one site is dependent
531 on the state at the other site. Because the null model is a general form of the alternative
532 model, both models can be compared under a likelihood ratio test (LRT) with degrees of
533 freedom (df) equal to the difference in the number of parameters between models. Because
534 the median branch length of the tree is 0.0019 substitutions per site, making multiple
535 changes at a single site or reversions to the ancestral state unlikely, we set the rates of
536 transition to the ancestral state to zero. After this restriction, the null independent model
537 had four free transition parameters. To test for dependence, we imposed two additional
538 restrictions to the model: one forcing the transition rate at site one to be fixed regardless of
539 the state of site 2 (q13=q24), and a second forcing the transition rate at site 2 to be fixed
540 regardless of the state of site 1 (q12=q34). This effectively tests whether the transition rate
541 is affected by the state of either site leaving the model with only two free transition
542 parameters (LRT with df=2). To run the analysis, the phylogeny branch lengths were scaled
543 using BayesTraits to have a mean length of 0.1; to increase the chance of finding the true
544 maximum likelihood, we set MLTries to 250.
545

References

1. Agrawal, A.A., Petschenka, G., Bingham, R.A., Weber, M.G., and Rasmann, S. (2012). Toxic cardenolides: chemical ecology and coevolution of specialized plant–herbivore interactions. New Phytologist *194*, 28-45.
2. Mohammadi, S., Yang, L., Bulbert, M., and Rowland, H.M. (2022). Defence mitigation by predators of chemically defended prey integrated over the predation sequence and across biological levels with a focus on cardiotonic steroids. Royal Society Open Science *9*, 220363.
3. Horisberger, J.-D. (2004). Recent insights into the structure and mechanism of the sodium pump. Physiology *19*, 377-387.
4. Lingrel, J.B., Orlowski, J., Shull, M.M., and Price, E.M. (1990). Molecular genetics of Na, K-ATPase. Progress in nucleic acid research and molecular biology *38*, 37-89.
5. Siegel, R.B., Taylor, R., Saracco, J.F., Helton, L., and Stock, S. (2016). GPS-tracking reveals non-breeding locations and apparent molt migration of a Black-headed Grosbeak. Journal of Field Ornithology *87*, 196-203.
6. Fink, L.S., and Brower, L.P. (1981). Birds Can Overcome the Cardenolide Defense of Monarch Butterflies in Mexico. Nature *291*, 67-70.
7. Fink, L.S., Brower, L.P., Waide, R.B., and Spitzer, P.R. (1983). Overwintering Monarch Butterflies as Food for Insectivorous Birds in Mexico. Biotropica *15*, 151-153.
8. Brower, L.P., and Calvert, W.H. (1985). Foraging dynamics of bird predators on overwintering monarch butterflies in Mexico. Evolution *39*, 852-868.
9. Li, F., Weng, Y., Wang, L., He, H., Yang, J., and Tang, X. (2010). The efficacy and safety of bufadienolides-loaded nanostructured lipid carriers. International Journal of Pharmaceutics *393*, 204-212.
10. Li, W., Lin, X., Yang, Z., Zhang, W., Ren, T., Qu, F., Wang, Y., Zhang, N., and Tang, X. (2015). A bufadienolide-loaded submicron emulsion for oral administration: stability, antitumor efficacy and toxicity. International Journal of Pharmaceutics *479*, 52-62.
11. Ferreira, P.M.P., de Sousa, L.Q., de Sousa, R.W.R., de Jesus Rodrigues, D., dos Santos Monção Filho, E., Chaves, M.H., Júnior, G.M.V., dos Santos Rizzo, M., Filgueiras, L.A., and Mendes, A.N. (2023). Toxic profile of marinobufagin from poisonous Amazon toads and antitumoral effects on human colorectal carcinomas. Journal of ethnopharmacology *310*, 116406.
12. Jurowski, K., Niżnik, Ł., Frydrych, A., Kobylarz, D., Noga, M., Krośniak, A., Fijałkowska, O., Świdniak, A., and Ahuja, V. (2025). Toxicological profile of Acovenoside A as an active pharmaceutical ingredient – prediction of missing key toxicological endpoints using in silico toxicology methodology. Chemico-Biological Interactions *408*, 111404.
13. Marty, M.A. (1983). METABOLISM AND DISPOSITION OF MILKWEED (ASCLEPIADACEAE) CARDENOLIDES IN MONARCH BUTTERFLY LARVAE, DANAUS PLEXIPPUS, AND IN A PREDATOR, PEROMYSCUS MANICULATUS. (United States -- California: University of California, Davis), p. 222.
14. Whiteman, N.K., and Mooney, K.A. (2012). Insects converge on resistance. Nature *489*, 376-377.
15. Groen, S.C., and Whiteman, N.K. (2021). Convergent evolution of cardiac-glycoside resistance in predators and parasites of milkweed herbivores. Curr Biol *31*, R1465-r1466.

16. Mohammadi, S., Herrera-Álvarez, S., Yang, L., Rodriguez-Ordonez, M.d.P., Zhang, K., Storz, J.F., Dobler, S., Crawford, A.J., and Andolfatto, P. (2022). Constraints on the evolution of toxin-resistant Na, K-ATPases have limited dependence on sequence divergence. PLoS genetics *18*, e1010323.
17. Mohammadi, S., Savitzky, A.H., Lohr, J., and Dobler, S. (2017). Toad toxin-resistant snake (Thamnophis elegans) expresses high levels of mutant Na+/K+-ATPase mRNA in cardiac muscle. Gene *614*, 21-25.
18. Mohammadi, S., Yang, L., Harpak, A., Herrera-Álvarez, S., del Pilar Rodríguez-Ordoñez, M., Peng, J., Zhang, K., Storz, J.F., Dobler, S., and Crawford, A.J. (2021). Concerted evolution reveals co-adapted amino acid substitutions in Na+ K+-ATPase of frogs that prey on toxic toads. Current Biology *31*, 2530-2538. e2510.
19. Ujvari, B., Mun, H.-c., Conigrave, A.D., Bray, A., Osterkamp, J., Halling, P., and Madsen, T. (2013). Isolation breeds naivety: island living robs Australian varanid lizards of toad-toxin immunity via four-base-pair mutation. Evolution *67*, 289-294.
20. Ujvari, B., Casewell, N.R., Sunagar, K., Arbuckle, K., Wüster, W., Lo, N., O'Meally, D., Beckmann, C., King, G.F., and Deplazes, E. (2015). Widespread convergence in toxin resistance by predictable molecular evolution. Proceedings of the National Academy of Sciences *112*, 11911-11916.
21. Mohammadi, S., Gompert, Z., Gonzalez, J., Takeuchi, H., Mori, A., and Savitzky, A.H. (2016). Toxin-resistant isoforms of Na+/K+-ATPase in snakes do not closely track dietary specialization on toads. Proceedings of the Royal Society B: Biological Sciences *283*, 20162111.
22. Marshall, B.M., Casewell, N.R., Vences, M., Glaw, F., Andreone, F., Rakotoarison, A., Zancolli, G., Woog, F., and Wüster, W. (2018). Widespread vulnerability of Malagasy predators to the toxins of an introduced toad. Current Biology *28*, R654-R655.
23. Karageorgi, M., Groen, S.C., Sumbul, F., Pelaez, J.N., Verster, K.I., Aguilar, J.M., Hastings, A.P., Bernstein, S.L., Matsunaga, T., Astourian, M., et al. (2019). Genome editing retraces the evolution of toxin resistance in the monarch butterfly. Nature *574*, 409-412.
24. Taverner, A.M., Yang, L., Barile, Z.J., Lin, B., Peng, J., Pinharanda, A.P., Rao, A.S., Roland, B.P., Talsma, A.D., and Wei, D. (2019). Adaptive substitutions underlying cardiac glycoside insensitivity in insects exhibit epistasis in vivo. Elife *8*.
25. Carpenter, G.H. (1942). Observations and experiments in Africa by the late CFM Swynnerton on wild birds eating butterflies and the preference shown. In Proceedings of the Linnean Society of London, Volume 154. (Oxford University Press), pp. 10-46.
26. Brodie, J.F. (2017). Evolutionary cascades induced by large frugivores. Proceedings of the National Academy of Sciences *114*, 11998-12002.
27. Agrawal, A.A., Hastings, A.P., Lenhart, P.A., Blecher, M., Duplais, C., Petschenka, G., Hawlena, D., Wagschal, V., and Dobler, S. (2024). Convergence and Divergence among Herbivorous Insects Specialized on Toxic Plants: Revealing Syndromes among the Cardenolide Feeders across the Insect Tree of Life. The American Naturalist *204*, 201-220.
28. Dobler, S., Dalla, S., Wagschal, V., and Agrawal, A.A. (2012). Community-wide convergent evolution in insect adaptation to toxic cardenolides by substitutions in the Na,K-ATPase. Proceedings of the National Academy of Sciences *109*, 13040-13045.

29. Dalla, S., and Dobler, S. (2016). Gene duplications circumvent trade-offs in enzyme function: Insect adaptation to toxic host plants. Evolution *70*, 2767-2777.
30. Lee, M.S., Cau, A., Naish, D., and Dyke, G.J. (2014). Morphological clocks in paleontology, and a mid-Cretaceous origin of crown Aves. Systematic Biology *63*, 442-449.
31. Stiller, J., Feng, S., Chowdhury, A.-A., Rivas-González, I., Duchêne, D.A., Fang, Q., Deng, Y., Kozlov, A., Stamatakis, A., Claramunt, S., et al. (2024). Complexity of avian evolution revealed by family-level genomes. Nature *629*, 851-860.
32. Brower, L.P., Nelson, C.J., Seiber, J.N., Fink, L.S., and Bond, C. (1988). Exaptation as an alternative to coevolution in the cardenolide-based chemical defense of monarch butterflies (*Danaus plexippus L.*) against avian predators. In Chemical mediation of coevolution, K.C. Spencer, ed. (London: Harcourt Brace Jovanovich).
33. Groen, S.C., and Whiteman, N.K. (2021). Convergent evolution of cardiac-glycoside resistance in predators and parasites of milkweed herbivores. Current Biology *31*, R1465-R1466.
34. Petschenka, G., Fandrich, S., Sander, N., Wagschal, V., Boppré, M., and Dobler, S. (2013). Stepwise evolution of resistance to toxic cardenolides via genetic substitutions in the Na+/K+-ATPase of milkweed butterflies (Lepidoptera: Danaini). Evolution *67*, 2753-2761.
35. Mohammadi, S., Özdemir, H., Ozbek, P., Sumbul, F., Stiller, J., Deng, Y., Crawford, A.J., Rowland, H.M., Storz, J.F., Andolfatto, P., et al. (2022). Epistatic Effects Between Amino Acid Insertions and Substitutions Mediate Toxin resistance of Vertebrate Na+,K+-ATPases. Mol Biol Evol *39*.
36. Yang, L., Ravikanthachari, N., Mariño-Pérez, R., Deshmukh, R., Wu, M., Rosenstein, A., Kunte, K., Song, H., and Andolfatto, P. (2019). Predictability in the evolution of Orthopteran cardenolide insensitivity. Philosophical Transactions of the Royal Society B *374*, 20180246.
37. Dobler, S., Wagschal, V., Pietsch, N., Dahdouli, N., Meinzer, F., Romey-Glüsing, R., and Schütte, K. (2019). New ways to acquire resistance: imperfect convergence in insect adaptations to a potent plant toxin. Proceedings of the Royal Society B: Biological Sciences *286*, 20190883.
38. Feng, S., Stiller, J., Deng, Y., Armstrong, J., Fang, Q., Reeve, A.H., Xie, D., Chen, G., Guo, C., and Faircloth, B.C. (2020). Dense sampling of bird diversity increases power of comparative genomics. Nature *587*, 252-257.
39. Crawford, N.G., Faircloth, B.C., McCormack, J.E., Brumfield, R.T., Winker, K., and Glenn, T.C. (2012). More than 1000 ultraconserved elements provide evidence that turtles are the sister group of archosaurs. Biology letters *8*, 783-786.
40. Crawford, N.G., Parham, J.F., Sellas, A.B., Faircloth, B.C., Glenn, T.C., Papenfuss, T.J., Henderson, J.B., Hansen, M.H., and Simison, W.B. (2015). A phylogenomic analysis of turtles. Molecular phylogenetics and evolution *83*, 250-257.
41. Green, R.E., Braun, E.L., Armstrong, J., Earl, D., Nguyen, N., Hickey, G., Vandewege, M.W., St. John, J.A., Capella-Gutiérrez, S., and Castoe, T.A. (2014). Three crocodilian genomes reveal ancestral patterns of evolution among archosaurs. Science *346*, 1254449.
42. Katoh, K., and Standley, D.M. (2013). MAFFT multiple sequence alignment software version 7: improvements in performance and usability. Mol Biol Evol *30*, 772-780.

43. Minh, B.Q., Schmidt, H.A., Chernomor, O., Schrempf, D., Woodhams, M.D., Von Haeseler, A., and Lanfear, R. (2020). IQ-TREE 2: new models and efficient methods for phylogenetic inference in the genomic era. Molecular biology and evolution *37*, 1530-1534.
44. Hanson-Smith, V., Kolaczkowski, B., and Thornton, J.W. (2010). Robustness of ancestral sequence reconstruction to phylogenetic uncertainty. Molecular biology and evolution *27*, 1988-1999.
45. Jarvis, E.D., Mirarab, S., Aberer, A.J., Li, B., Houde, P., Li, C., Ho, S.Y.W., Faircloth, B.C., Nabholz, B., Howard, J.T., et al. (2014). Whole-genome analyses resolve early branches in the tree of life of modern birds. Science *346*, 1320-1331.
46. Prum, R.O., Berv, J.S., Dornburg, A., Field, D.J., Townsend, J.P., Lemmon, E.M., and Lemmon, A.R. (2015). A comprehensive phylogeny of birds (Aves) using targeted next-generation DNA sequencing. Nature *526*, 569-573.
47. Jetz, W., Thomas, G.H., Joy, J.B., Hartmann, K., and Mooers, A.O. (2012). The global diversity of birds in space and time. Nature *491*, 444-448.
48. Scholz, J., and Suppmann, S. (2017). A new single-step protocol for rapid baculovirus-driven protein production in insect cells. BMC biotechnology *17*, 1-9.
49. Löptien, J., Vesting, S., Dobler, S., and Mohammadi, S. (2024). Evaluating the efficacy of protein quantification methods on membrane proteins. Open Biology *14*, 240082.
50. Taussky, H.H., and Shorr, E. (1953). A microcolorimetric method for the determination of inorganic phosphorus. J Biol chem *202*, 675-685.
51. Pagel, M., and Meade, A. (2006). Bayesian analysis of correlated evolution of discrete characters by reversible-jump Markov chain Monte Carlo. The American Naturalist *167*, 808-825.